Supplementary Information

Non-Kekulé Copolymer Films for Optoelectronics

Niannian Wu[1,2], Nobuhiko Mitoma[1,2,*], Shunsuke Mori[1], Yi Ling Chiew[1], Xiuzhen Yu[1], Yugo Oshima[3], Shuxu Wang[1,2], Jinxu Liu[1,2], and Takuzo Aida[1,2,*]

1. RIKEN Center for Emergent Matter Science, 2-1 Hirosawa, Wako, Saitama 351-0198, Japan.
2. Department of Chemistry and Biotechnology, The University of Tokyo, 7-3-1 Hongo, Bunkyo-ku, Tokyo 113-8656, Japan.
3. RIKEN Cluster for Pioneering Research, 2-1 Hirosawa, Wako, Saitama 351-0198, Japan.

*Corresponding authors: nobuhiko.mitoma@riken.jp, aida@macro.t.u-tokyo.ac.jp

Table of Contents

1. Materials

Unless otherwise noted, all commercial reagents were used as received. Melamine was purchased from Nacalai Tesque, Inc. D(+)-glucose was purchased from Kanto Chemical Co., Inc. Target substrates (***i.e.***, micro slide glass) for vapor deposition polymerization (VDP) were purchased from Matsunami Glass Ind., Ltd. They were cut into a designated size before use. It was ultrasonically cleaned in acetone, ethanol, and high-purity water for 10 min and dried using nitrogen gas before use.

Preparation of slide glass substrates

Substrates were meticulously cleaned as follows: first, they were sonicated in acetone, 2-propanol, and high-purity water for 10 min, and dried with nitrogen gas before use. Finally, to complete the cleaning process, they underwent UV–ozone treatment for 15 min.

Synthesis of gCN-*co*-gC films

gCN films were synthesized using a homemade VDP system with a 1-inch quartz tube. In a typical gCN fabrication process, a slide glass substrate with an area of 25 mm × 25 mm was horizontally positioned in the central region of furnace 2 (right side, high-temperature zone) in the VDP system. A 13.5-mL glass vial containing 1 g of melamine was placed at the center of furnace 1 (left side, low-temperature zone), as shown in Supplementary Fig. 1. Argon gas was flowed from the left to right of the quartz tube at a rate of 25 mL min^{-1}. The temperature in furnace 2 (***i.e.***, target substrate) was raised to 550 °C. Once the substrate reached 550 °C, melamine in furnace 1 was heated to 300°C and maintained for an additional 30 min. Then, substrates were kept for an additional 10 min at 550°C after the heating program in furnace 1 was completed. After heating and reaction processes, samples were allowed to rapidly cool to room temperature (~25 °C) and collected.

Synthesis of gCN-***co***-gC films via two-zone VDP is following. In a typical process, a 13.5-mL glass vial containing a mixture of melamine and glucose powders (1 g) was placed at the center of furnace 1 and a slide glass substrate was horizontally positioned in the center of furnace 2 (Supplementary Fig. 1). VDP

synthesis was initiated by increasing the temperature of furnace 2 to 550°C using argon as the carrier gas (flow rate = 25 mL min^{-1}). Once the temperature in furnace 2 reached 550°C, furnace 1 was heated to 250°C and maintained for an additional 30 min. Subsequently, the temperature of furnace 1 was further increased from 250°C to 400°C, and furnace 1 was maintained at 400°C for an additional 10 min. Similarly, furnace 2 was maintained at 550°C for an additional 10 min after the first oven heating program was completed. Upon the completion of synthesis, samples were allowed to rapidly cool to room temperature (~25 °C) and collected. The resulting films were a transparent brownish-yellow color.

Photoresponsive device fabrication

Photoresponsive devices were fabricated on glass substrates covered with gCN-***co***-gC (Supplementary Fig. 6). To fabricate the electrodes on gCN-***co***-gC, DC magnetron sputtering (nanoVDP-S10A, Moorfield Nanotechnology) was employed to deposit 100-nm-thick Ag on gCN-***co***-gC under vacuum ($<5 \times 10^{-5}$ Pa) using shadow masks. The channel length and width were 150 and 1000 μm, respectively. The fabricated photoresponsive device comprises the following layer sequence: glass/gCN-***co***-gC/Ag. The current to voltage (***I***–***V***) measurement was performed using a source meter (B2985B, Keysight).

2. Methods

gCN-***co***-gC films were prepared via VDP in a two-zone tube furnace. The electronic absorption spectra were recorded using a JASCO V-760 spectrophotometer. The fluorescence spectra were recorded using a Nikon ECLIPSE Ti2 spectrometer with a 40-nm excelsior diode laser controller (excited wavelength = 405 nm). X-ray photoelectron spectroscopy (XPS) was performed using a PHI 5000 Versa Probe II surface analysis instrument (ULVAC-PHI) and a Kratos Analytical AXIS-ULTRADLD spectrometer using a monochromatic Al Kα X-ray radiation. XPS spectra obtained were corrected using the C 1s peak of graphitic carbon at 284.8 eV. The XRD measurements along the out-of-plane direction were performed using a Philips X'Pert Pro Super X-ray diffractometer with Cu Kα radiation. SEM was performed using a scanning electron microscope (JSM-6700F, and 5 kV). Atomic-force microscopy (AFM) images were taken on an Oxford Instruments model Cypher system. HREM and scanning TEM with energy-dispersive X-ray spectroscopy (STEM-EDS) mapping analyses were performed using a multifunctional transmission electron microscope (JEOL JEM-2800) at an accelerating voltage of 200 kV, equipped with STEM-EDS. EPR spectra were recorded using a Bruker ESP 300E spectrometer. A solar simulator (HAL-320 Compact Xenon Light Source) equipped with an AM 1.5G filter was used as an external light source. For photocurrent measurements, photoresponsive devices were irradiated using a laser-driven light source (Energetiq, EQ-77-QZ-S) with a monochromator (Zolix Instruments, Omni-λ3047i). Electron paramagnetic resonance spectra were recorded using a Bruker ESP 300E spectrometer (resonance conditions used were 9.0–9.4 GHz). A solar simulator (HAL-320 Compact Xenon Light Source) equipped with an AM 1.5G filter was used as an external light source. The Nanoindentation experiments were carried out using an ENT-NEXUS (ELIONIX Inc.). Nanoindentations were performed under the load-control mode at 30 °C and humidity around 60 RH%. The gCN-***co***-gC films were fixed onto the measurement stage using TOAGOSEI-ARON ALPHA (cyano-acrylate hydrogen-based acrylates) to rigidly fix the specimens. A diamond indenter tip with a Berkovich geometry was used in the nanoindentation experiments. A maximum load value of 1 mN was applied and a

loading/unloading rate of 1.5 mN/s was used for all the experiments. The holding time at the maximum load was set to 5 s. Young's modulus was collected from recovery curves.

Reduced modulus and hardness of gCN-*co*-gC films by nanoindentation

gCN-***co***-gC film obtained by two-zone VDP onto a glass substrate was subjected to nanoindentation for obtaining its force-curve profile (Supplementary Fig. 12). Then, by analyzing the force-curve profile using well established methods, reduced modulus and hardness of 12 GPa and 1 GPa were obtained, respectively. The mechanical properties of both gCN and gCN-***co***-gC films were thoroughly examined using the nanoindentation technique. To estimate Young's modulus stiffness and hardness of the gCN-***co***-gC films accurately, a Berkovich nanoindenter was employed at various indentation depths (Fig. 5 in the main text). Careful attention was given to ensuring that the indentation depths remained shallow to minimize any substantial influence from the substrate, which was indeed detected at deeper penetration depths. When the indentation depth was between one-tenth to one-seventh of the thickness of the film, the influence of the substrate can be avoided. Therefore, these tests were not affected by the supporting substrate. By adopting this approach, the derived mechanical properties were more indicative of the film's intrinsic behavior. For the gCN-***co***-gC films, Young's modulus and hardness were stable, which also confirmed no influence of the supporting substrate.

3. Supplementary Figures

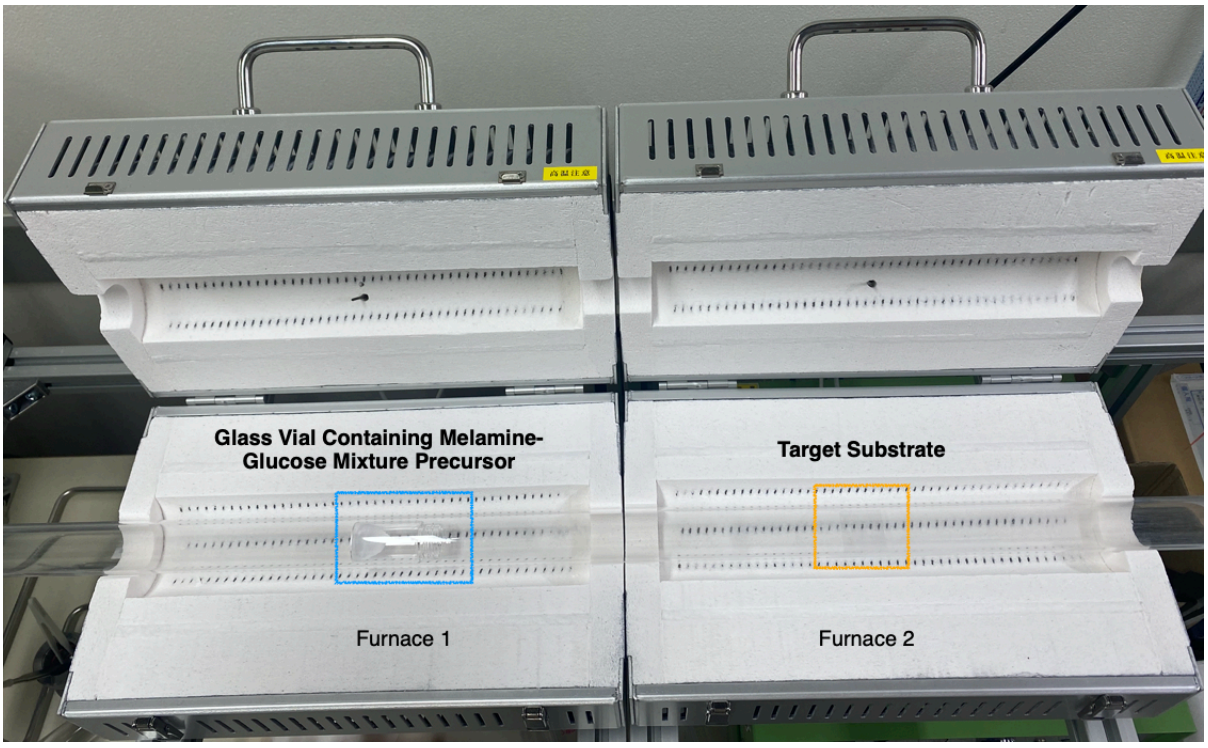

Supplementary Fig. 1| Photograph of the two-zone VDP setup to synthesize gCN-***co***-gC films using a melamine–glucose mixture as the precursor (surrounded by blue) and a target glass substrate (surrounded by orange).

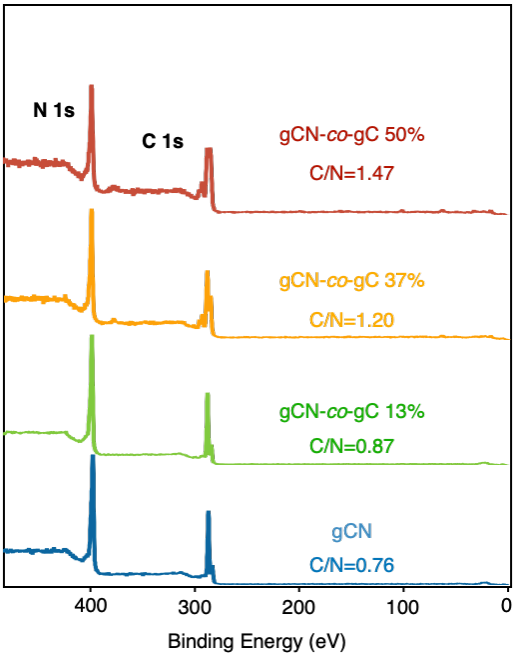

Supplementary Fig. 2| XPS survey spectra of gCN, gCN-***co***-gC 13%, 37%, and 50%.

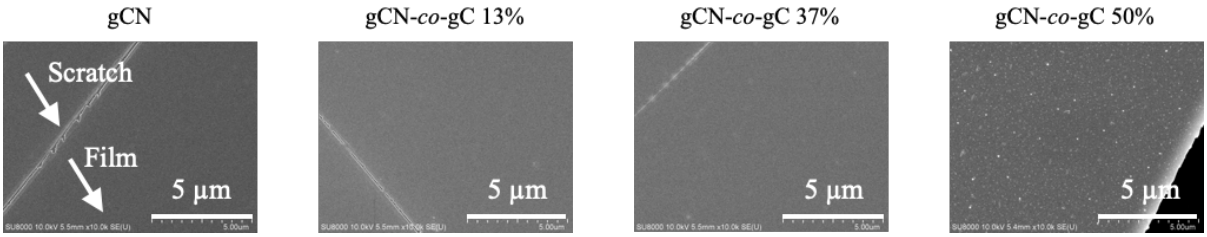

Supplementary Fig. 3| Top-view SEM images of gCN, gCN-***co***-gC 13%, 37% and 50% films obtained by VDP onto a glass substrate.

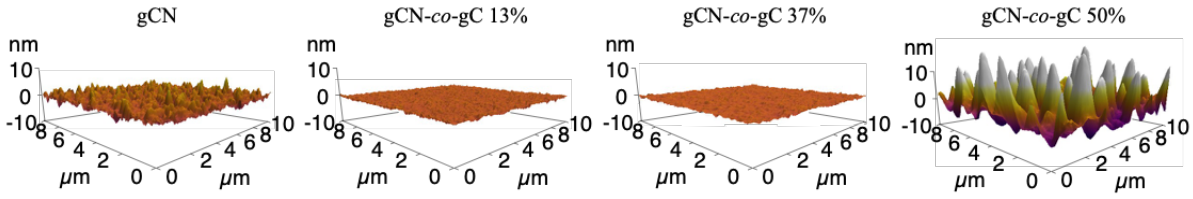

Supplementary Fig. 4| AFM images of gCN, gCN-***co***-gC 13%, 37%, and 50% films, showing a surface roughness of 0.8 nm, 0.4 nm, 0.3 nm, and 6 nm respectively.

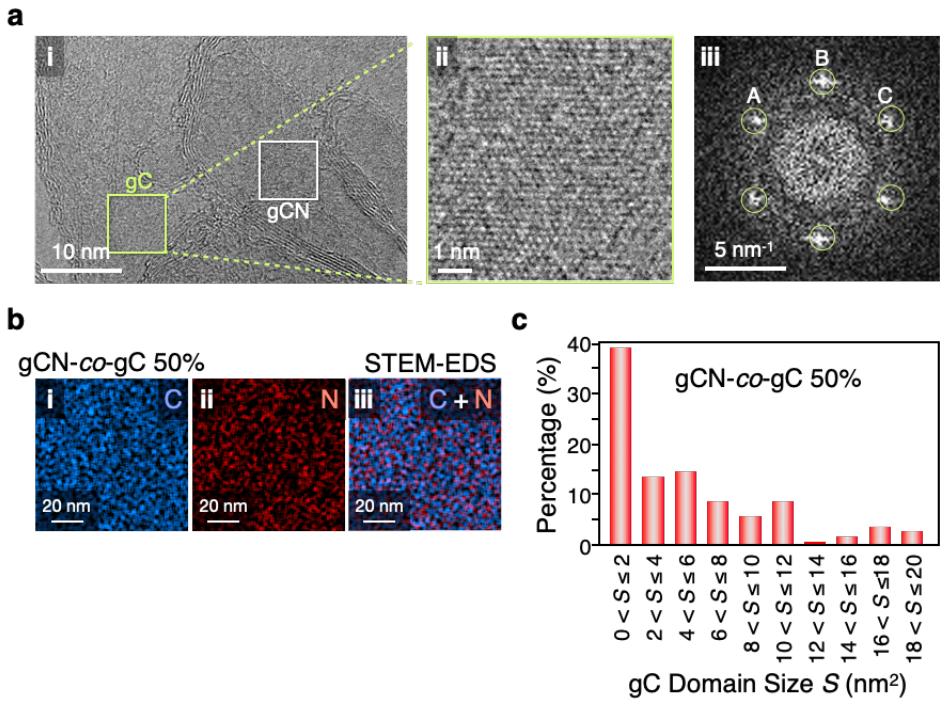

Supplementary Fig. 5| (**a**) HREM images (**i, ii**) and fast Fourier transform scans (**iii**) of gCN-***co***-gC 50% (d_A = 0.20 nm, d_B = 0.20 nm, d_c = 0.20 nm). (**b**) STEM-EDS C (**i**), N (**ii**), and C + N overlay mapping images (**iii**) of gCN-***co***-gC 50% films. (**c**) Histogram of the size distribution of the incorporated gC domains of gCN-***co***-gC 50%.

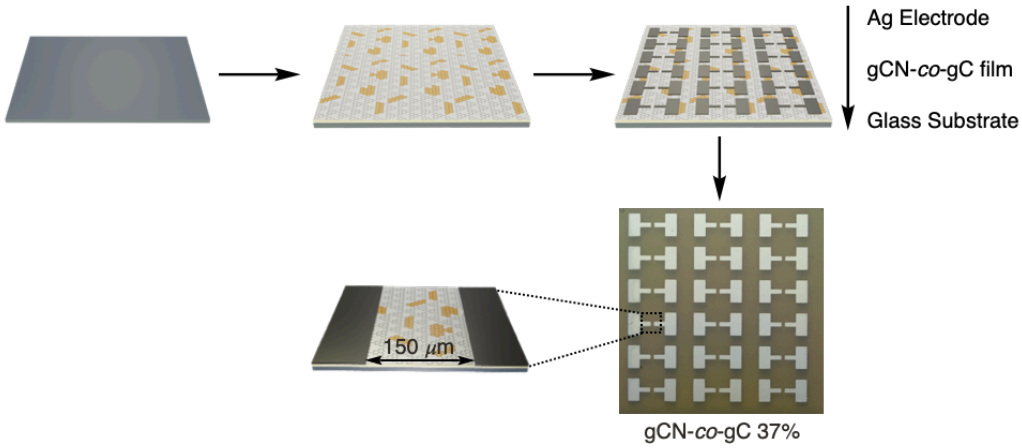

Supplementary Fig. 6| Schematic diagram of the fabrication of the gCN-***co***-gC photoresponsive device and the photograph of a photoresponsive device containing gCN-***co***-gC 37%.

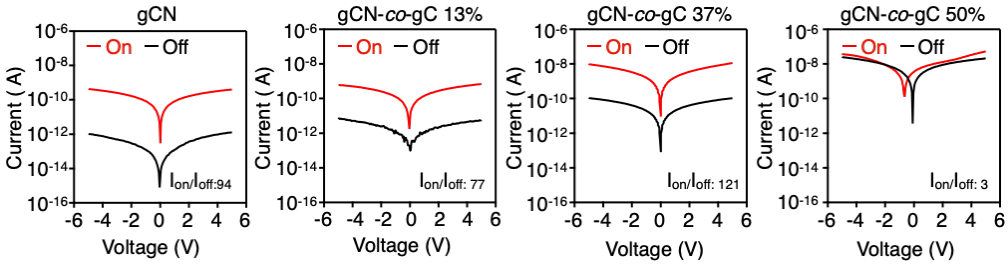

Supplementary Fig. 7| I-V curves of gCN, gCN-*co*-gC 13%, 37% and 50% films with light (365 nm, 75 mW cm^{-2}) irradiation and without light irradiation.

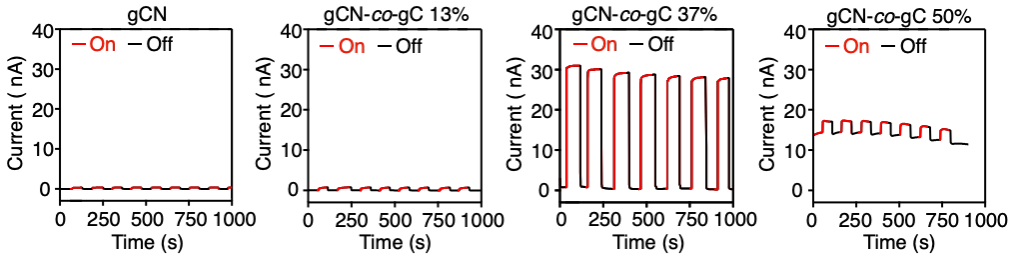

Supplementary Fig. 8| Cycle stability of the photocurrents of gCN, gCN-*co*-gC 13%, 37%, and 50% (365 nm, 75 mW cm^{-2}, bias: 5V).

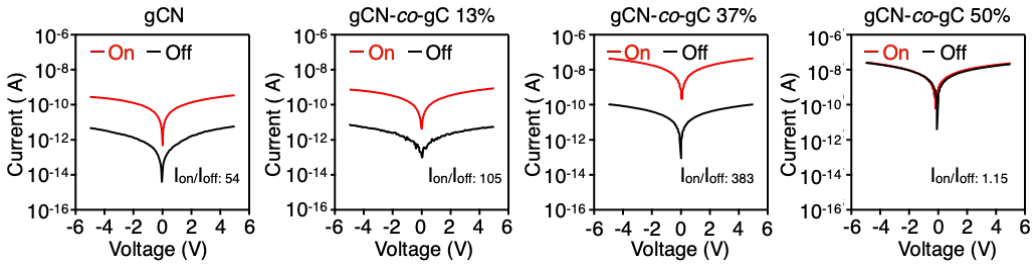

Supplementary Fig. 9| I-V curves of gCN, gCN-***co***-gC 13%, 37% and 50% films with light (420 nm, 120 mW cm^{-2}) irradiation and without light irradiation.

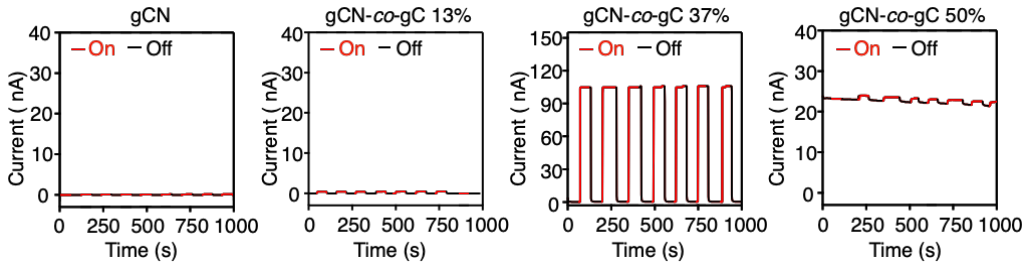

Supplementary Fig. 10| Cycle stability of the photocurrents of gCN, gCN-***co***-gC 13%, 37%, and 50% (420 nm, 120 mW cm^{-2}, bias: 5V).

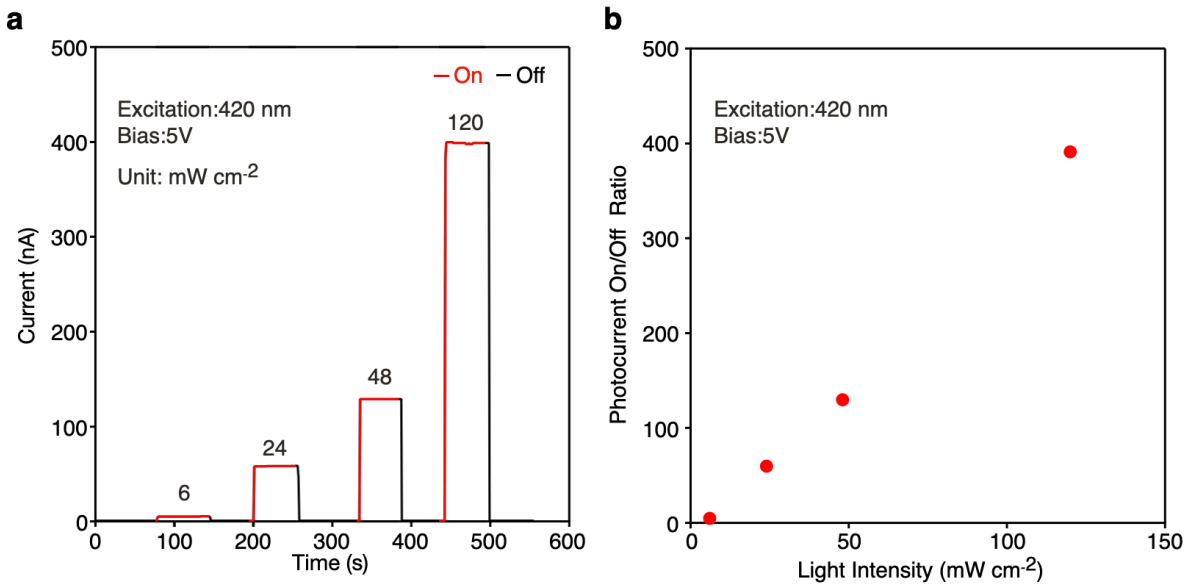

Supplementary Fig. 11| (**a**) Photocurrent of gCN-co-gC 37% upon light illumination. (**b**) Dependence of photocurrent on/off ratio as a function of the light illumination intensities.

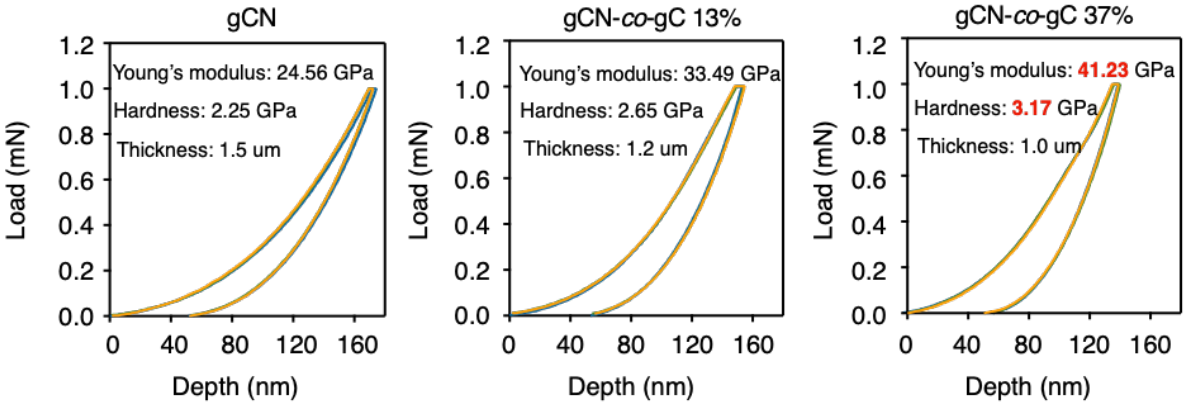

Supplementary Fig. 12| Force curve profiles of a gCN, gCN-*co*-gC 13%, and 37% films obtained by nanoindentation.

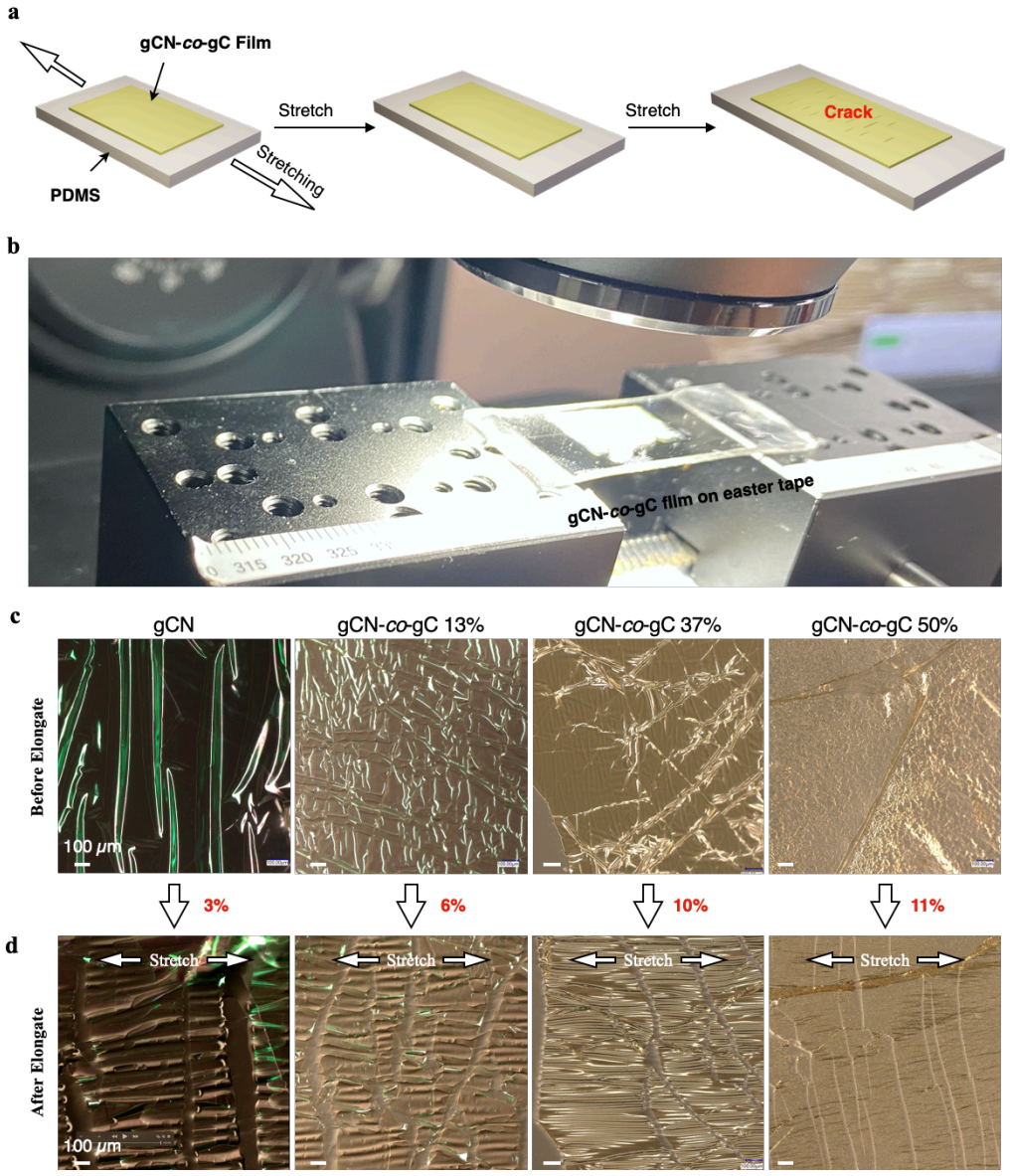

Supplementary Fig. 13| (**a**) Illustration of film on elastomer crack onset strain measurement. (**b**) Optical image of the experimental setup. (**c**) Microscope images before elongation and (**d**) a characteristic crack features observed in the measurements for gCN, gCN-***co***-gC 13%, 37%, and g 50% films after elongation. All images were captured near their respective crack onset strains. In all films, the strain was applied along the long axis of the page. The scale bar for all images is 100 μm.

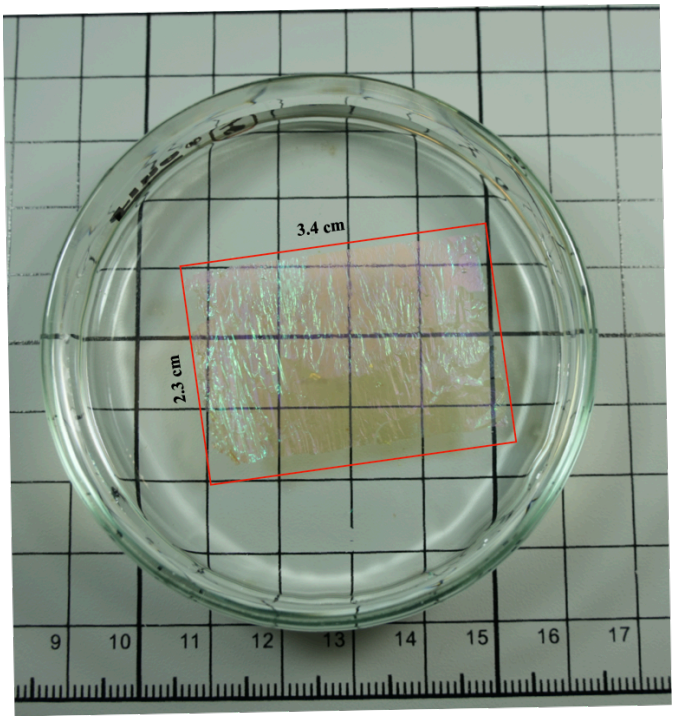

Supplementary Fig. 14| Large size freestanding gCN-***co***-gC 37% (500-nm-thick) film floats on water.

Supplementary Videos

Video S1: Freestanding gCN-***co***-gC 37% film (500-nm-thick) floats on water and shows flexibility.